Progress Report on NASA Grant: NGR 11-002-096

RESEARCH ON THE ELASTIC STABILITY of LARGE SHELLS

Principal Investigator: Professor Wilfred H. Horton

(NASA-CR-139665) RESEARCH ON THE ELASTIC STABILITY OF LARGE SHELLS Semiannual Progress Report (Georgia Inst. of Tech.) 18 p HC $4.00 CSCL 20K

N74-33360

Unclas

G3/32 47899

Considerable progress has been made on the large shell tests. The remaining three shells have all been completely instrumented, checked for circularity and surveyed for stiffness. One shell has been installed in the test facility and a series of preliminary load distribution checks have been made. These tests have indicated that we can now achieve a better distribution of stress in the central bays than in the prior tests. In fact at low load levels the stresses in the center bay were uniform around the shell to within $\pm$ 2.5%, and this degree of uniformity improves with increasing load. The degree of uniformity in the bays at either end of the shell was not of this degree of excellence although it was good in comparison with that normally accomplished. The difficulty experienced in smoothing this distribution and avoiding local bending actions in the lower regions is the lack of mating between the end surface of the shell and the loading device. We have made substantial progress in evaluating this discrepancy. For this purpose we have adopted plastigages, (perfect circle plastigage Type PG I clearance range .001 to .003 inch) made by Perfect Circle Hagerstown, Indiana. These devices are thin plastic rods which are inserted between the two surfaces whose degree of mating is in question. When the two surfaces are mated together the plastic gages are flattened by amounts which are related to the degree of fit. We have used some 250 measuring stations around the ends of the shell and from the flattening actions have been able to quantify the discrepancies. These discrepancies in fit are readily correlatable with the strain distributions measured. The shell is now being reworked to remove the high and low spots. Maximum discrepancy achieved in the preliminary end matching was of the order $\pm$ 2 thousandths, but the majority of the surface was much closer than this. We have removed the vehicle from the test frame and are now in the process of reducing this discrepancy. We are confident that we can achieve a tolerance of $\pm$ 1 thousandth, and with patience possible do somewhat better.

The stiffness surveys are most informative. We can readily detect the various frame joints and steps are being taken to modify the frame joints in such a manner as to produce a stronger joint which at the same time does not produce as substantial a local stiffness variation as is currently experienced. An analysis of the first shell test results leads us to the opinion that the instability load level in that test was marked, influenced by the ring behavior in the neighborhood of a lap joint. We feel certain that the changes which we have in mind will improve the shell performance.

The very detailed studies of initial shape which we have made give clear indication that the shell initial geometry is excellent. In the circumferential direction, for the vehicle now being readied for test, there is a dominant double wave and a six wave component which may well be due to the construction from six panels. The amplitudes are small however.

In the longitudinal direction the wave components higher than two contribute little to the deviation. In particular the wave components that might be associated with the prescence of eight frames are not of any appreciable magnitude. However, some of the longitudinal generators are much straighter than others.

The various sheets attached to this report give quantitative description of the remarks made heretofore.

Figure 1 portrays the distribution of strain achieved in the central and end regions, while Figure 2 shows the variation along vertical generators chosen at random. In Table 1 we present an analysis of the circumfrential deviation data and in Table II a similar analysis for the longitudinal information. The graphs of Figure 3 show the variation in stiffness around the frames of the shell and Figure 4 gives the mean stiffness distribution along the shell.

Stiffness contour maps and deviation contour maps are in the course of preparation but are not included here.

Some changes in the basic testing method have been made. The 72 hydraulic jacks which were used in prior work have been replaced by 18 larger jacks and the multiplicity of ground steel plates which were used between the jack ends and the base of the shell have been replaced by one heavy ring. These changes were made to (1) ease the many alignment problems (2) to improve the lower end load distribution. There is little doubt that these objectives have been met, but the attainment of a flat contact surface on this ring presented considerable difficulties since no local contractor could be found to fabricate the ring to our exacting requirement.

There seems, from tests which we have conducted, little doubt that the effects of the small descrepancies between the machined ends of the shells and the upper and lower end loading rings could readily be mitigated by the use of Devcon A, Plastic Steel. (Devcon Corporation, Danvers, Massachusetts, 01923). However, it is our considered opinion that its use would involve more work than is entailed in the adjustment process which we are adopting, since the two end rings would require special surfacing for each test. The surfacing of these rings is a long and tedious process since no machine shop in the area has appropriate tools.

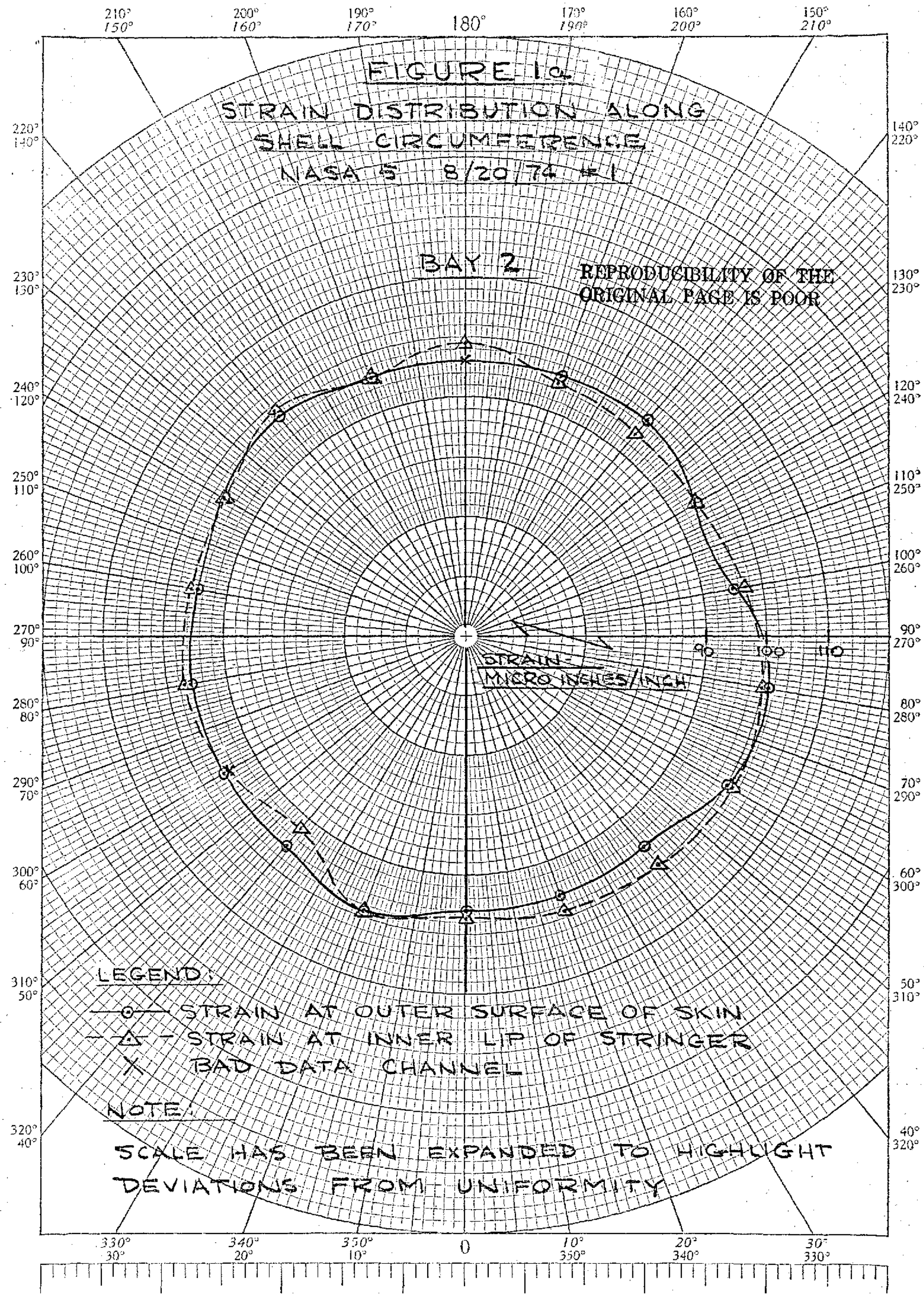
FIGURE 1a
STRAIN DISTRIBUTION ALONG
SHELL CIRCUMFERENCE
NASA 5 8/20/74 #1
BAY 2
STRAIN-
MICRO INCHES/INCH
90
100
110
LEGEND:
STRAIN AT OUTER SURFACE OF SKIN
STRAIN AT INNER LIP OF STRINGER
BAD DATA CHANNEL
NOTE:
SCALE HAS BEEN EXPANDED TO HIGHLIGHT
DEVIATIONS FROM UNIFORMITY
180°
0

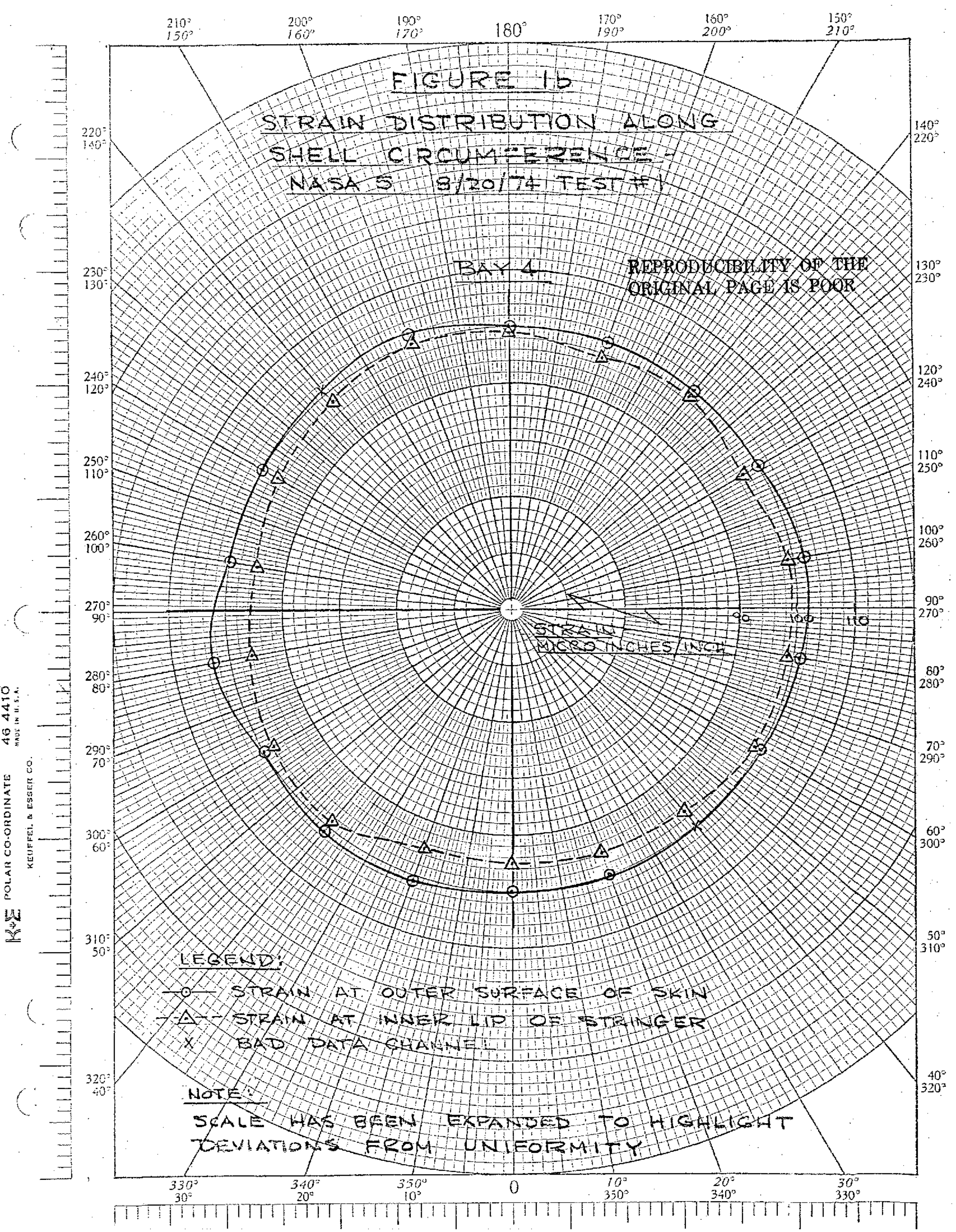
FIGURE 1b
STRAIN DISTRIBUTION ALONG
SHELL CIRCUMFERENCE -
NASA 5 8/20/74 TEST #1
BAY 4
STRAIN
MICRO INCHES/INCH
90
100
110
LEGEND:
STRAIN AT OUTER SURFACE OF SKIN
STRAIN AT INNER LIP OF STRINGER
X BAD DATA CHANNEL
NOTE:
SCALE HAS BEEN EXPANDED TO HIGHLIGHT
DEVIATIONS FROM UNIFORMITY
KEUFFEL & ESSER CO.
POLAR CO-ORDINATE 46 4410
MADE IN U.S.A.

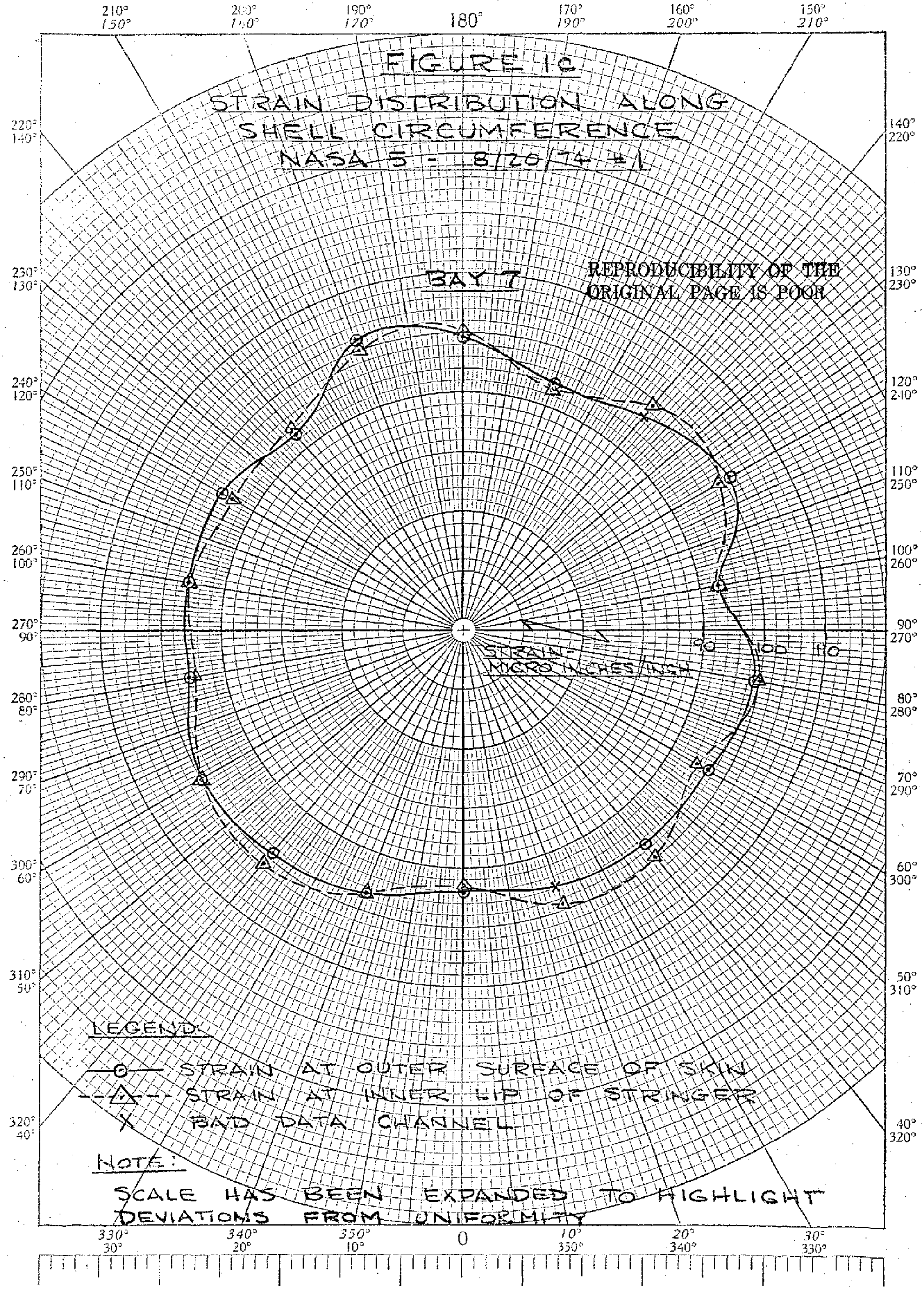
FIGURE 1c
STRAIN DISTRIBUTION ALONG
SHELL CIRCUMFERENCE
NASA 5 - 8/20/74 #1
BAY 7
REPRODUCIBILITY OF THE ORIGINAL PAGE IS POOR
STRAIN-MICRO INCHES/INCH
90
100
110
LEGEND:
STRAIN AT OUTER SURFACE OF SKIN
STRAIN AT INNER LIP OF STRINGER
BAD DATA CHANNEL
NOTE:
SCALE HAS BEEN EXPANDED TO HIGHLIGHT DEVIATIONS FROM UNIFORMITY
POLAR CO-ORDINATE
KEUFFEL & ESSER CO.

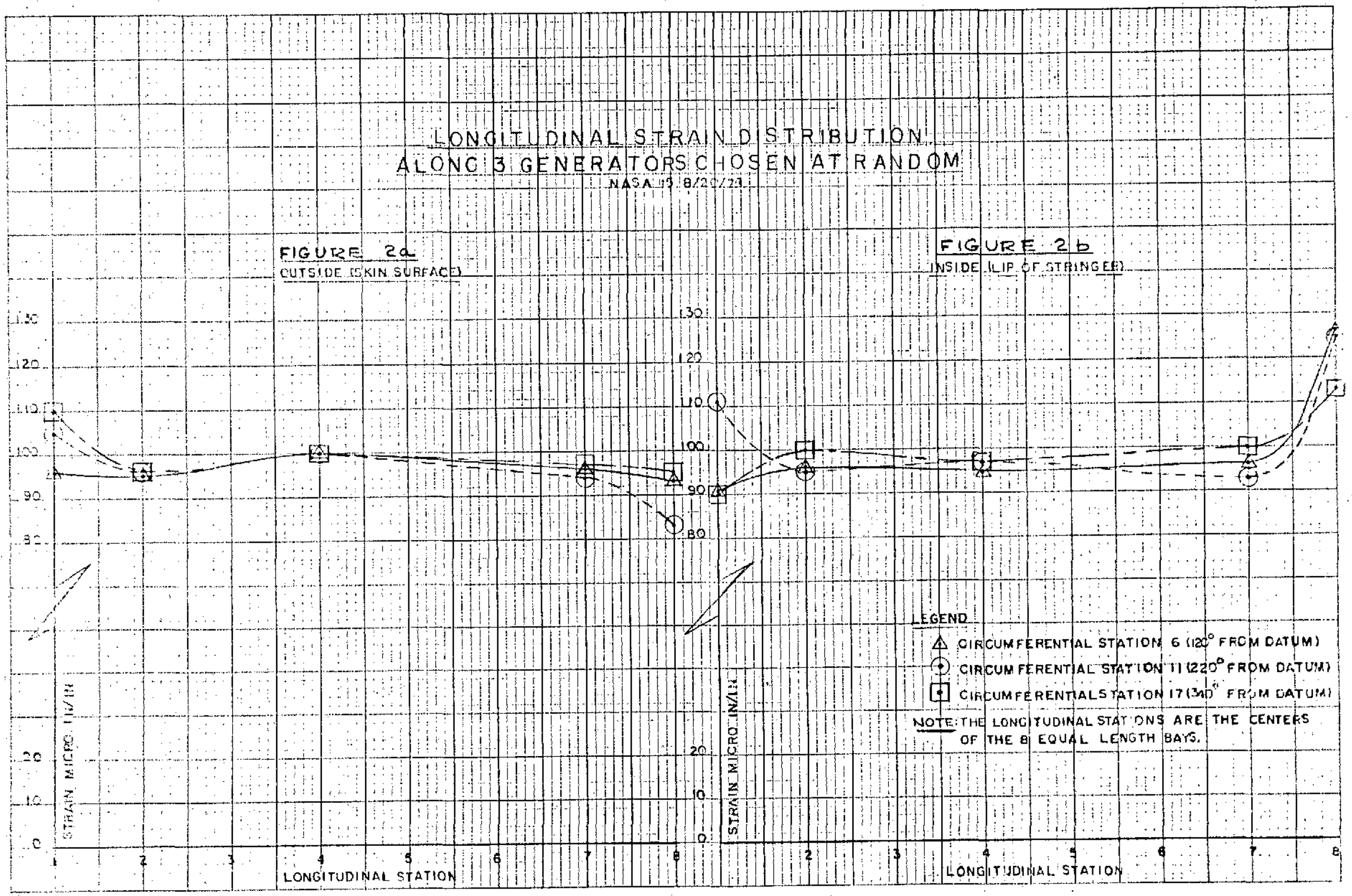
LONGITUDINAL STRAIN DISTRIBUTION
ALONG 3 GENERATORS CHOSEN AT RANDOM
FIGURE 2a
OUTSIDE (SKIN SURFACE)
FIGURE 2b
INSIDE (LIP OF STRINGER)
STRAIN MICRO IN/IN
LONGITUDINAL STATION
LEGEND
CIRCUMFERENTIAL STATION 6 (120° FROM DATUM)
CIRCUMFERENTIAL STATION 11 (220° FROM DATUM)
CIRCUMFERENTIAL STATION 17 (340° FROM DATUM)
NOTE: THE LONGITUDINAL STATIONS ARE THE CENTERS OF THE 8 EQUAL LENGTH BAYS.

FIGURE 3a

NASA SHELL 5 VARIATION IN STIFFENESS AROUND RINGS 1, 2, 3, 4

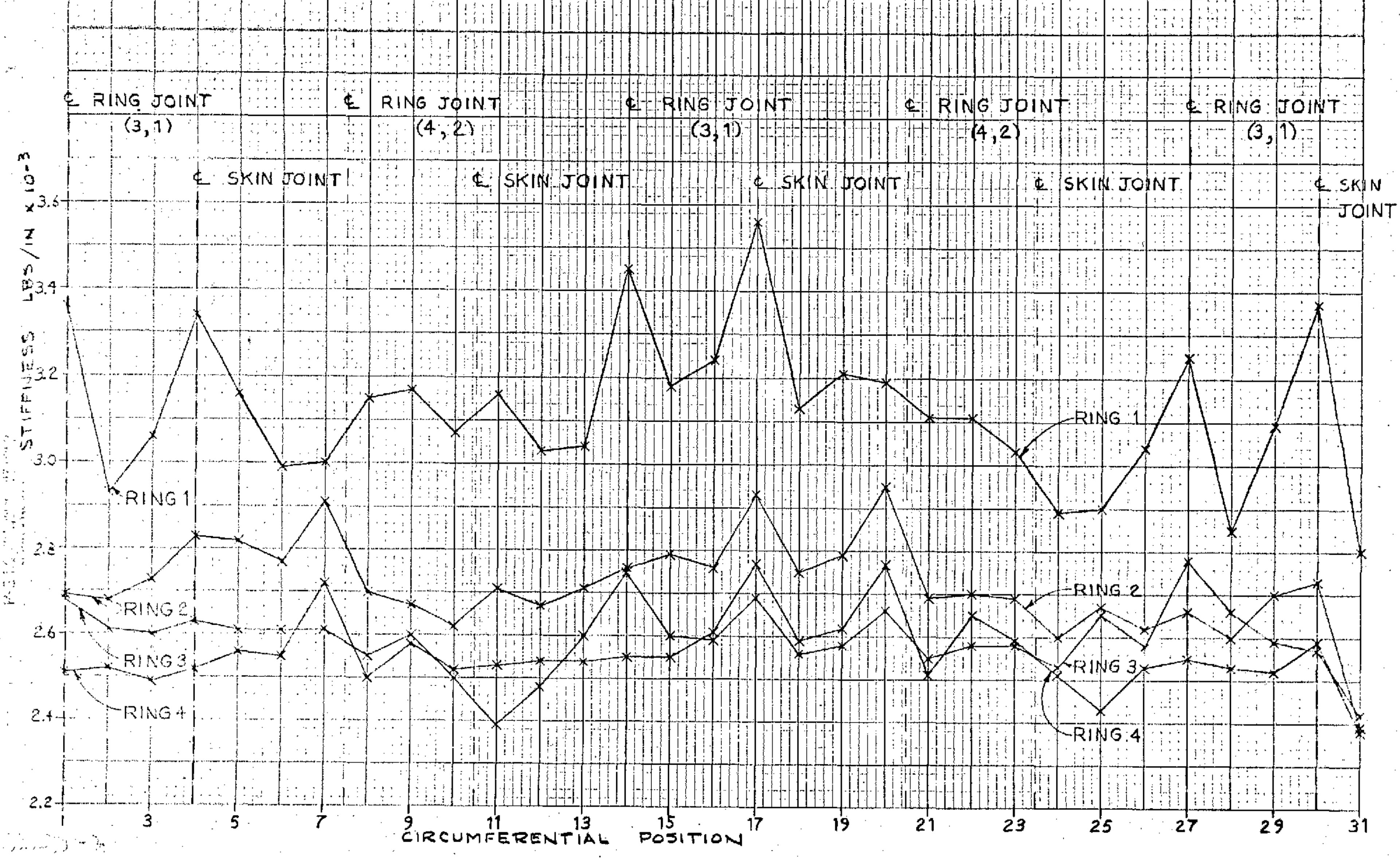

FIGURE 3a (CONT'D)

NASA SHELL 5 VARIATION IN STIFFNESS AROUND RINGS 1,2,3,4

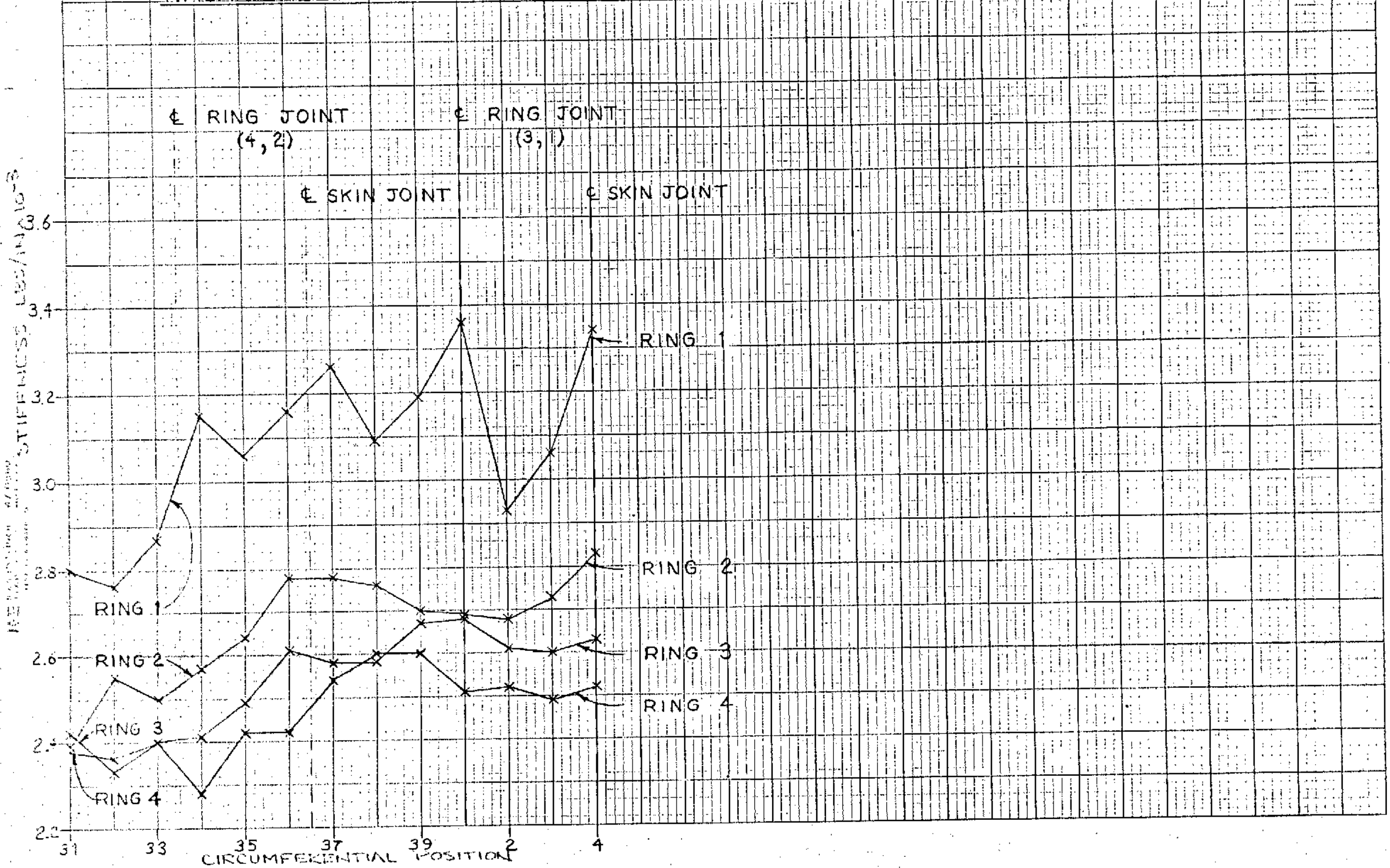

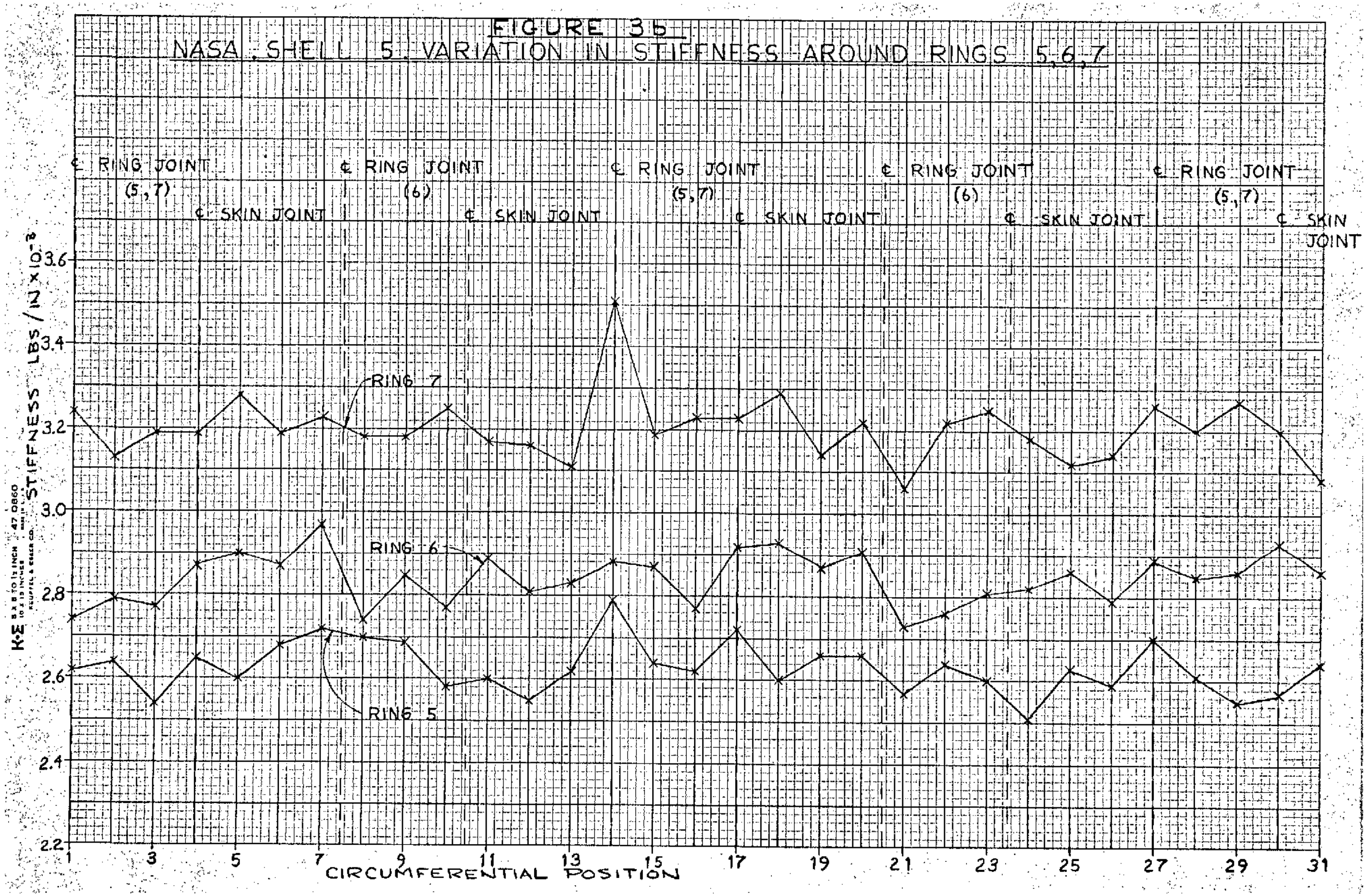

FIGURE 35
NASA, SHELL 5, VARIATION IN STIFFNESS AROUND RINGS 5,6,7
℄ RING JOINT (5,7)
℄ RING JOINT (6)
℄ RING JOINT (5,7)
℄ RING JOINT (6)
℄ RING JOINT (5,7)
℄ SKIN JOINT
℄ SKIN JOINT
℄ SKIN JOINT
℄ SKIN JOINT
℄ SKIN JOINT
RING 7
RING 6
RING 5
STIFFNESS LBS/IN × 10⁻³
3.6
3.4
3.2
3.0
2.8
2.6
2.4
2.2
1
3
5
7
9
11
13
15
17
19
21
23
25
27
29
31
CIRCUMFERENTIAL POSITION
K+E

FIGURE 3b (CONT'D)
NASA SHELL 5. VARIATION IN STIFFNESS AROUND RINGS 5,6,7

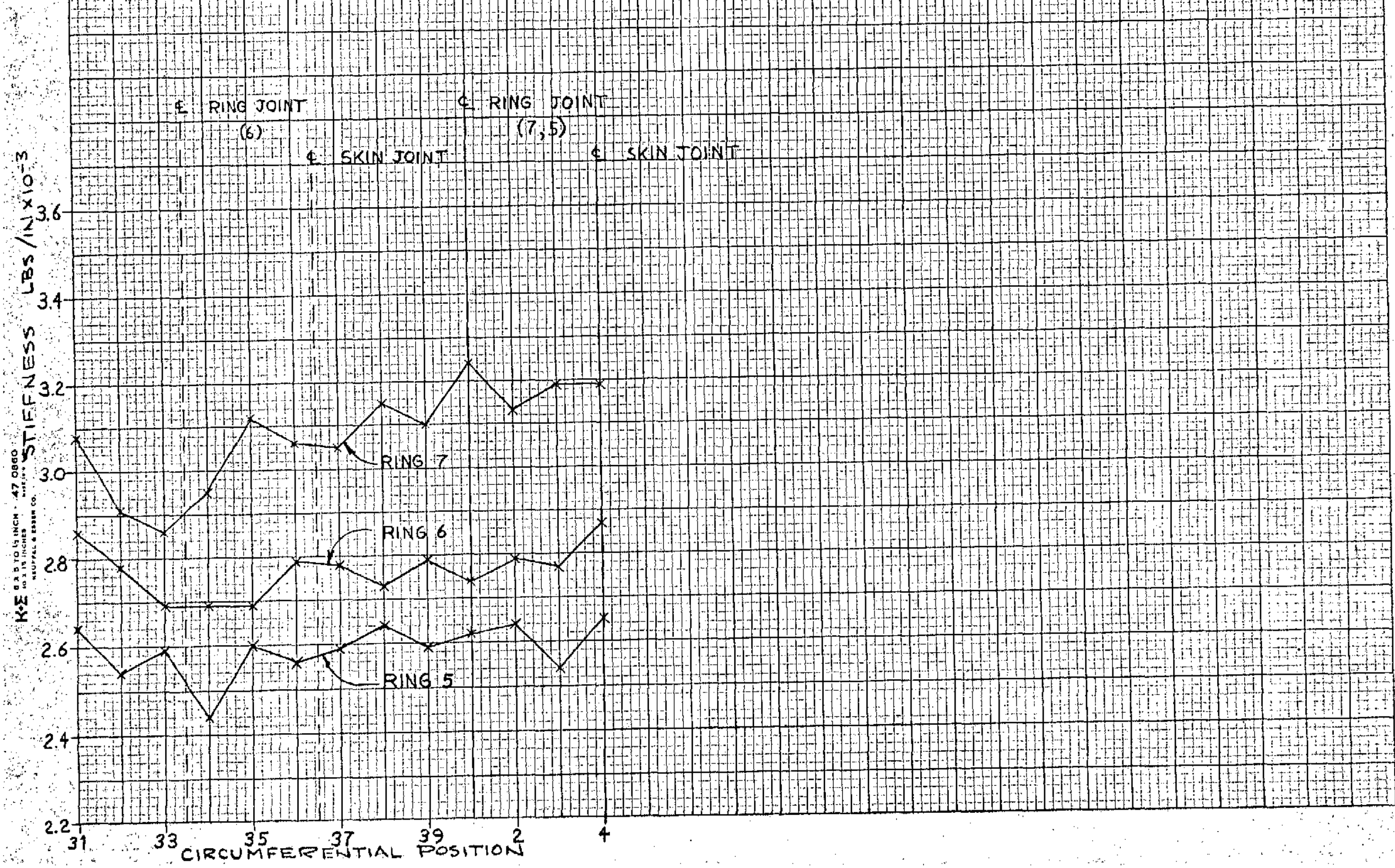

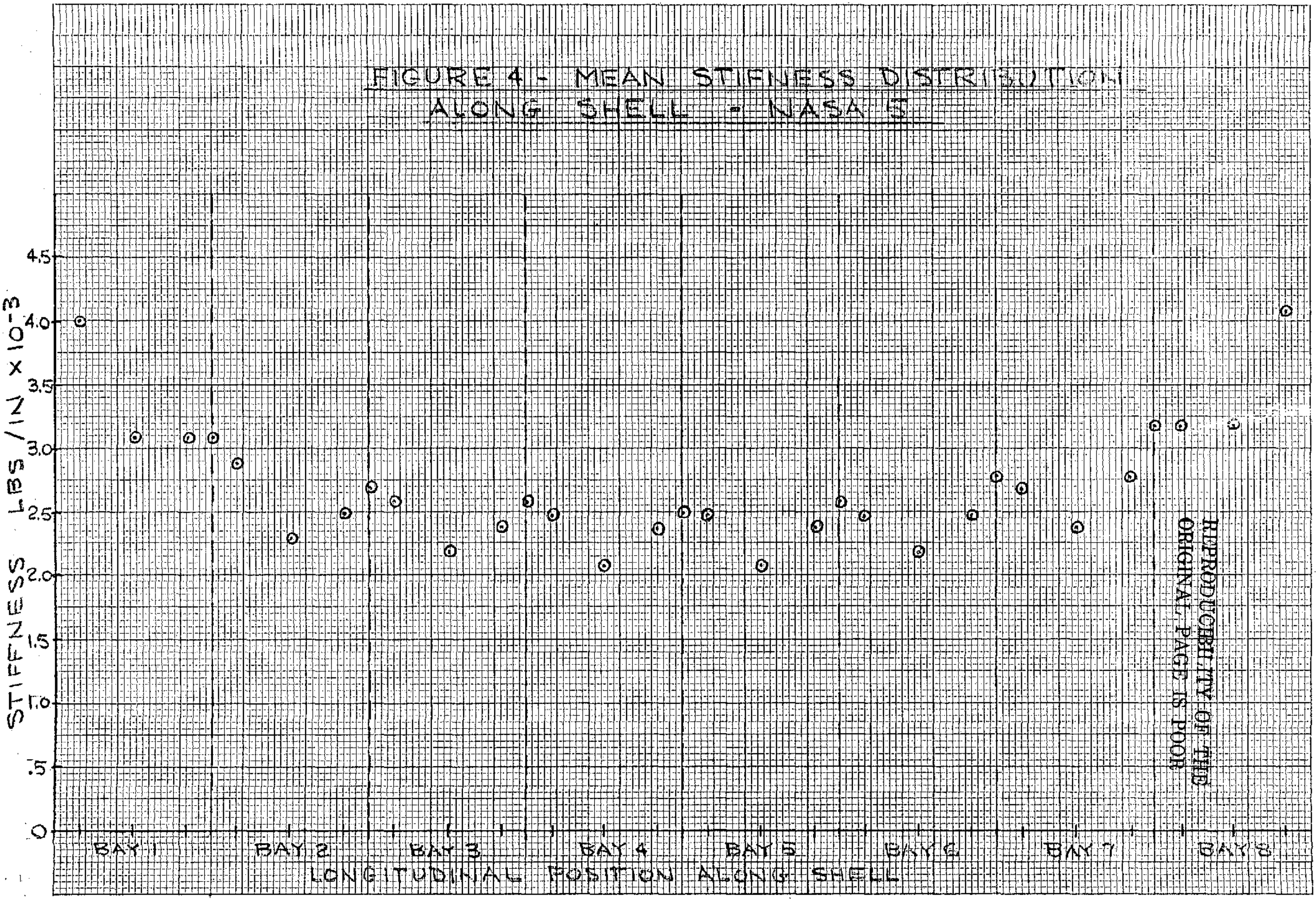
FIGURE 4 - MEAN STIFFNESS DISTRIBUTION
ALONG SHELL - NASA 5
STIFFNESS LBS/IN x 10-3
4.5
4.0
3.5
3.0
2.5
2.0
1.5
1.0
.5
0
BAY 1
BAY 2
BAY 3
BAY 4
BAY 5
BAY 6
BAY 7
BAY 8
LONGITUDINAL POSITION ALONG SHELL

Table I

FOURIER SERIES COEFFICIENTS FOR DEVIATION DATA (CIRCUMFERENTIAL)

BAY = 1 POSITION = 4

# OF WAVES	AMPLITUDE (MILS)
0	-30.5
1	4.4
2	55.9
3	5.8
4	1.9
5	2.5
6	6.4
7	.8
8	1.8
9	1.5
10	1.7

BAY = 2 POSITION = 17.5

# OF WAVES	AMPLITUDE (MILS)
0	-23.9
1	.9
2	56.6
3	9.5
4	.9
5	3.2
6	11.9
7	2.1
8	3
9	4.6
10	2.5

BAY = 3 POSITION = 31

# OF WAVES	AMPLITUDE (MILS)
0	-11.6
1	2.7
2	56.1
3	12.1
4	3.8
5	3.8
6	11.1
7	1.5
8	2.4
9	4.7
10	3.8

BAY = 4 POSITION = 38.5

# OF WAVES	AMPLITUDE (MILS)
0	-8.6
1	3.6
2	56
3	13.2
4	4.6
5	3.5
6	10.1
7	1.7
8	2.4
9	3.2
10	2.8

Table I Continued

BAY = 4 POSITION = 44.5

# OF WAVES	AMPLITUDE (MILS)
Ø	-6.4
1	4.1
2	56.5
3	13.9
4	5.2
5	3
6	1Ø.2
7	2.1
8	2.3
9	1.5
1Ø	1.7

BAY = 4 POSITION = 5Ø.5

# OF WAVES	AMPLITUDE (MILS)
Ø	.6
1	4
2	57
3	14.9
4	5.6
5	3
6	1Ø.2
7	2.5
8	2.8
9	1
1Ø	2.3

BAY = 5 POSITION = 58

# OF WAVES	AMPLITUDE (MILS)
Ø	5.1
1	4.3
2	56.8
3	15.9
4	6.3
5	2.8
6	11
7	2.8
8	3
9	1.8
1Ø	4.5

BAY = 6 POSITION = 71.5

# OF WAVES	AMPLITUDE (MILS)
Ø	17.7
1	2.9
2	56.8
3	17.6
4	6.9
5	2.2
6	14.6
7	2.7
8	2
9	2.3
1Ø	5

Table I Continued

BAY = 7 POSITION = 85

# OF WAVES	AMPLITUDE (MILS)
0	22.5
1	1.3
2	56.6
3	17.1
4	5.8
5	.6
6	12.2
7	2.7
8	1.6
9	1.4
10	2.2

BAY = 8 POSITION = 97

# OF WAVES	AMPLITUDE (MILS)
0	15.7
1	5
2	56.1
3	15.9
4	3
5	1.2
6	6.9
7	1.1
8	1.6
9	.7
10	.7

Table II

FOURIER SERIES COEFFICIENTS FOR DEVIATION DATA (LONGITUDINAL)

9 DEGREES

# OF WAVES	AMPLITUDE
Ø	19.5
1	23.1
2	11
3	7
4	4.9
5	3.8
6	3.5
7	3.8
8	3.3
9	2.8
1Ø	2.5

53 DEGREES

# OF WAVES	AMPLITUDE
Ø	-18.5
1	4Ø
2	16.3
3	12
4	6.9
5	5.6
6	5.1
7	4.8
8	4.3
9	3.5
1Ø	3.3

99 DEGREES

# OF WAVES	AMPLITUDE
Ø	-38.9
1	15.8
2	1Ø.8
3	4.9
4	2.5
5	2.2
6	2.1
7	2.7
8	2.4
9	1.5
1Ø	1.6

143 DEGREES

# OF WAVES	AMPLITUDE
Ø	32
1	8.1
2	6.9
3	3.7
4	.9
5	1.2
6	.9
7	2.1
8	1.7
9	.9
1Ø	1.2

Table II Continued

189 DEGREES

# OF WAVES	AMPLITUDE
Ø	44.7
1	33.2
2	14.3
3	8.3
4	5.2
5	4.7
6	4.2
7	4
8	3.5
9	2.9
1Ø	2.9

233 DEGREES

# OF WAVES	AMPLITUDE
Ø	-38.5
1	32.6
2	15.3
3	1Ø.5
4	6
5	4.8
6	4.4
7	4.5
8	4.1
9	3.4
1Ø	3.3

279 DEGREES

# OF WAVES	AMPLITUDE
Ø	-4Ø.6
1	1Ø.8
2	6.9
3	3.2
4	2.1
5	2.1
6	1.7
7	2.2
8	2.3
9	1.3
1Ø	1.6

323 DEGREES

# OF WAVES	AMPLITUDE
Ø	51.2
1	28.9
2	9.8
3	3.9
4	3.4
5	2.8
6	2.6
7	2.6
8	2.6
9	2.1
1Ø	2.1